

# Computational Study on Transcutaneous Frontal Nerve Stimulation: Simplification of Human Head Model

E. Salkim, A. N. Shiraz, A. Demosthenous, Department of Electronic and Electrical Engineering, University College London, Torrington Place, WC1E 7JE, London, UK.  
{E-mail: enver.salkim.14; a.shiraz; a.demosthenous@ucl.ac.uk}

**Abstract-** Migraine is a highly disabling disorder of the brain which may affect patients both socially and economically. The pharmaceutical and invasive treatment methods may have undesirable side effects and associated risks. It has recently been shown that transcutaneous supraorbital neuromodulation may suppress episodic migraine attacks. However, results have indicated low efficacy. This inconclusive response may be associated with neuro-anatomical variations in patients which may be investigated using computational models. Model complexity is a limiting factor in implementing such techniques. This paper investigates the effect of model complexity on fiber activation estimates in transcutaneous frontal nerve stimulation. It is shown that the model can be simplified while minimally affecting the outcome.

**Keywords—** Computational models, frontal nerve, migraine, neuromodulation.

## I. INTRODUCTION

Migraine is a neurological disorder which affects nearly 15% of the population [1] and costs the European community about €27 billion each year [2]. Its symptoms may be categorized as attacks of often severe throbbing head pain with sensory sensitivity of light and sound [3]. It is mainly related to the trigeminal nerve, the supraorbital nerve (SON) and the supratrochlear nerve (STN) which arise from the frontal branch of the ophthalmic division of the trigeminal nerve [4].

The available pharmaceutical treatments and invasive neuromodulation techniques are not completely effective due to their troublesome side-effects [5], [6]. Among different transcutaneous electrical nerve stimulation (TENS) methods, transcutaneous supraorbital nerve stimulation (tSNS) has been applied on a large group of people who have episodic migraine using a device called Cefaly (Cefaly, CEFALY Technology, Liège, Belgium). However, nearly 50% of this population were not satisfied. Therefore, it is assumed that this limited efficacy may be associated with the neuro-anatomical variations across different subjects. Therefore, using computational models of human head tissues, the

This work was funded by a PhD scholarship to E. Salkim by the Turkish Government, Ministry of National Education, and Mus Alpaslan University.

electrode patch and stimulator may be readily investigated to estimate current thresholds in neuromodulation therapy. These thresholds were investigated in a previous study using the simplified nerve and head model [7] shown in Fig. 1a. The present study aims to generate a highly detailed human head model to investigate the effect of model complexity on stimulus current threshold estimates. Both studies will be compared regarding stimulus current level and efficacy of model computation

The rest of the paper is organized as follows. Section II details the methods for generating the multilayer head volume conductor and computational models and the subsequent investigations. The percentage activation estimates of nerve fibers are reported in Section III. Discussion and conclusions outlining future directions are presented in Section IV.

For all the subsequent simulations and operations, a computer with an Intel Core i7-6700 CPU @ 3.4 GHz with 64 GB RAM was used.

## II. METHODS

### A. 3D MRI derived FEM model

A three dimensional (3D) model of human head was derived from magnetic resonance imaging (MRI) scans. The dataset was composed of 350 slices, each of which comprised of  $480 \times 480$  pixels. Voxel dimensions were  $0.5 \times 0.5 \times 0.5$  mm for each of the x, y and z planes [8]. The raw image data slices were smoothed and the main tissue layers were identified as a new gray scale value in MATLAB v.R2015b (MathWorks, Inc., Natic M, USA) for simplified human head model. Then, the new image data was exported to Simpleware ScanIP (Synopsys, Mountain View, USA) for further processing [7], as summarized in Fig.1a.

For the more realistic human head model, different head tissue layers (sixteen tissue layers) were segmented (a process in which the tissue layers are identified based on the gray scale data) based on in-built segmentation tools and smoothing algorithms of Simpleware ScanIP as shown in Figure 1b. However, the more realistic SON and STN nerve trajectories were extracted based on literature [9], [10] and

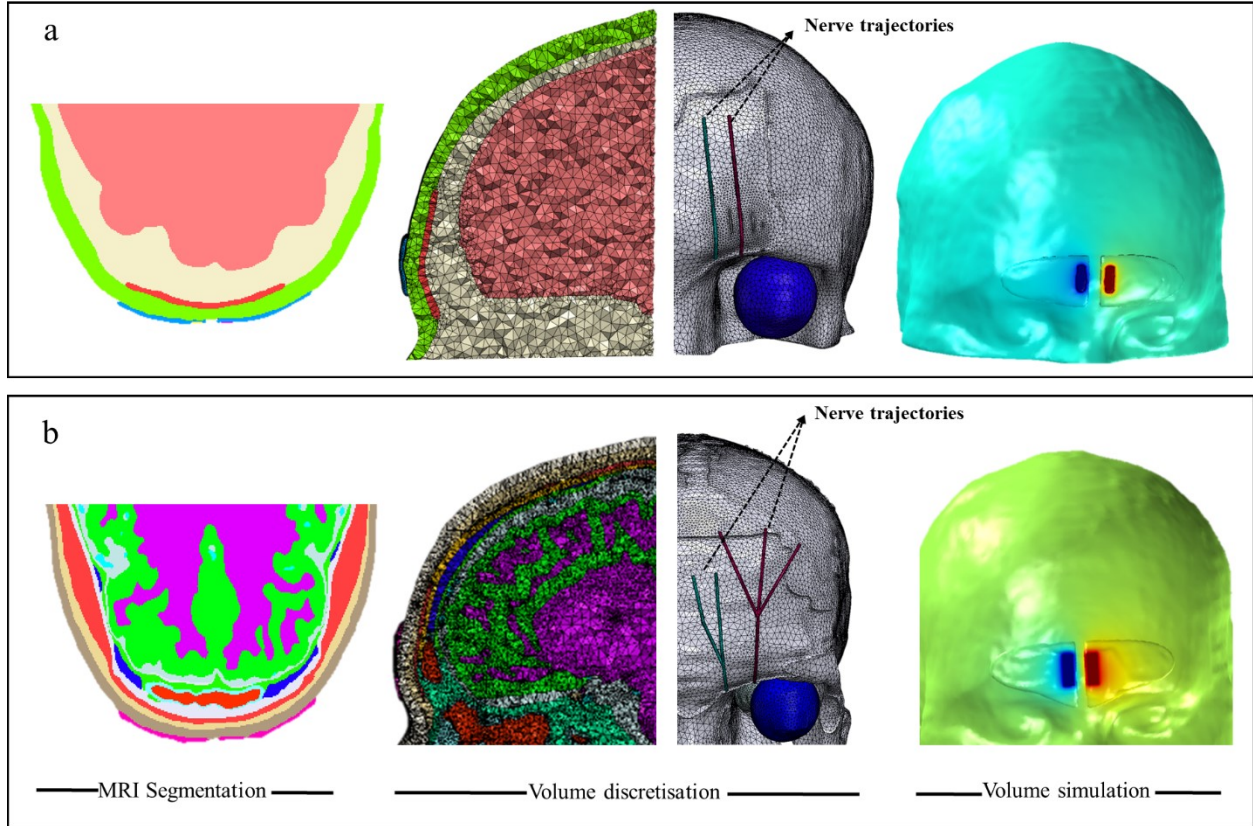


**Figure 1.** Comparing the simplified and more realistic human model, **a** shows the simplified model which is constructed from a few tissue layers, each nerve trajectory is represented with a branch, **b** shows the more detailed model which is built from sixteen tissue layers. The SON and STN were represented with red and green, respectively.

together with Cefaly's electrode patch were modeled from geometric shapes for both models. A Delaunay refinement approach was used to generate a tetrahedral mesh from the segmentation of head models. The features of human head models, based on computing, are summarized in Table II.

The volumetric mesh was generated from the segmented data which was then exported to COMSOL Multiphysics® for simulation.

### B. Computational models

As underlying differential equations cannot be solved analytically for complicated geometries (such as head volume conductor), finite element method (FEM) was used to solve for the electrical potential distribution in each medium. The simulations were carried out using COMSOL Multiphysics® while considering the quasi-static approximation of Maxwell equations demonstrated by Laplace equation as shown in (3). The exact methods of applying such formulations in COMSOL Multiphysics® are mentioned here. In the AC/DC Module of COMSOL,

*Electric Currents* physics in *Stationary* setting was selected.

$$\mathbf{J} = \sigma \cdot \mathbf{E} + \mathbf{J}_e \quad (1)$$

$$\nabla \cdot \mathbf{J} = Q_j \quad (2)$$

$$\nabla \cdot (\sigma \nabla V) = 0 \quad (3)$$

where  $n$  is the unit vector normal to the boundary,  $\mathbf{J}$  is current density,  $Q_j$  is the current source,  $\mathbf{E}$  is the electric field and  $\mathbf{J}_e$  is the external current density. By setting (2) and  $\mathbf{J}_e$  in (1) to zero everywhere in the model in *Electrical Currents* settings, a quasi-static was implemented by obtained (3). In COMSOL, *Terminal1* was set an anode and a current level of 1 mA was assigned in both models. *Terminal2* was set as cathode and -1 mA current level was applied.

A sphere was defined around the model [7] with specific conductivity ( $\sigma = 1e-10$  S/m) and Dirichlet boundary condition ( $V = 0$ ) was applied to its boundaries as an approximation of ground at infinity.

**Table I** Tissue conductivities

Tissue layers	Conductivity (S/m)	Reference
Skin	0.22	[13], [14]
Fat	0.025	[15]
Muscle	0.16	[15]
Nerve	1.2	[15]
Eyeball	0.5	[15]
Skull	0.015	[16]
CSF,S. sinuses	1.8	[17]
White matter	0.12	[18]
Gray matter (Brain)	0.1	[15]
Gel	0.1	-

The conductivity of other layers was set as listed in Table I.

In the *study* section in COMSOL, for an efficient solution of the TES finite element equation system, the algebraic multigrid preconditioned conjugate gradient iterative solver method was used with a relative tolerance of  $1 \times 10^{-6}$ . In the *results* section in COMSOL, the electrical potentials on the central nerve fibers of SON and STN were saved as extracellular potentials.

The cable model of mammalian nerve fiber was used to obtain percentage activation (PA) of nerve fibers [11]. Fibre distributions and the number of compartments and their geometric positions along the nerve length were designed based on our previous study [7]. The obtained electrical voltages in COMSOL were exported into Neuron v7.4 [12] to form voltage pulses; they were then applied to a population of the double layer cable model of mammalian fibers to simulate responses of fibres [7].

The PA of fibers was measured based on the fifth current pulse with the Cefaly stimulator parameters (biphasic symmetrical rectangular 250  $\mu$ s pulses at 60 Hz) [7]. The nerve fibers were divided from **node0** to **node25**. The PAs were firstly calculated for node0 for 100 fibers and then rechecked with node25, some PAs are shown in Figure 2 and 3. For the models in this study the fiber activations at 10% and 50% were identified. The simplified and more realistic head models are referred to as **SM** and **RM**, respectively, in the following results.

### III. RESULTS

The PAs of different nerve branches for different stimulus currents for RM and SM are shown in Figure 2 and 3, respectively.

**Table II** Comparison of the features of two computational models, IOARM is in-out aspect ratio for mean, IOARm is in-out aspect ratio for minimum

Features	SM	RM
Number of elements	1.4 million	22 million
Segmentation time	5 days	8 days
Discretization time	4.5 hours	26 hours
Simulation time	2min 11s	10 min 46s
Mesh quality	IOARM=0.77 IOARm=0.01	IOARM=0.73 IOARm=0.008

Although STN has multiple branches in RM and single branch in SM, the PAs with respect to stimulus current level are nearly identical. To stimulate around 50% of fibers, 5.3 mA is required for STN in the SM. Due to STN composed of two branches in RM, there are two stimulus current threshold levels to activate the same PA level. These are 5mA for right branch and 4.8 mA for left branch. To stimulate all fibers of STN in SM, 7.1 mA stimulus current is needed. However, to activate all fibers of STN in RM, 6.5 mA is required for both right and left branches of STN in RM.

For the case of SON, to stimulate the nerve fibers around 50%, 13 mA stimulation current was needed for all branches of RM. However, 50% of fibers can be stimulated by 12 mA for SM. Using 14.1 mA stimulus current can activate all nerve fibers of SON in SM. However, to stimulate all fibers of SON in the RM, the activation current thresholds were different for all branches. These levels are 16, 16.1 and 17 mA for right, centre and left branches, respectively.

### IV. DISCUSSION AND CONCLUSION

The objective of this study was to investigate the impact of highly detailed whole human head model on the stimulus current level for migraine neuromodulation therapy. In order to quantify this, FEM models were constructed to calculate the electric potential distributions in the volume due to bipolar electrode configuration. Then, the electric potential on the nerve fiber in the volume conductor was simulated as extracellular potential which was then fed to the multi-compartment cable models to simulate the response of the nerve to this stimulus.

Although the detailed head model was composed of more tissue layers than the simplified head model, the simulation results showed that there is not a significant difference between stimulus threshold current levels. A high level of the stimulus current was required to activate SON possibly as its trajectory is

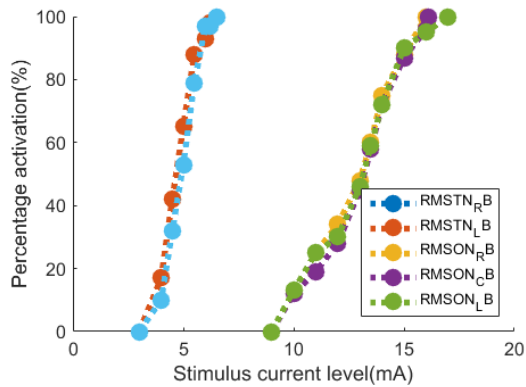


**Figure 2.** The PAs of nerve fibers of realistic model, RM (realistic model), RB (right branch), LB (left branch), and CB (center branch).

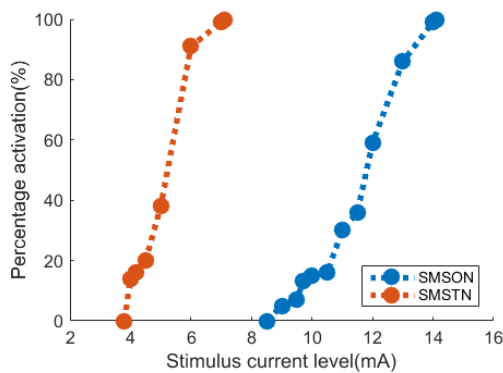


**Figure 3.** The PAs of nerve fibers of simplified model

placed deeper compared to STN. The difference between SM and RM in terms of stimulus threshold level may be due to the mesh size in the RM, because it was coarse meshed due to much more complexity to save time. This is a limitation of this study which should be rectified to generate variations of this model.

## References

[1] C. Manifestations, “migraine— current understanding and treatments,” vol. 346, no. 4, pp. 257–270, 2002.  
 [2] P. Andlin-Sobocki and W. Rössler, “Cost of psychotic disorders in Europe,” *Eur. J. Neurol.*, vol. 12, no. SUPPL. 1, pp. 74–77, 2005.  
 [3] C. Road, “The International Classification of Headache Disorders, 3rd edition (beta version),” *Cephalalgia*, vol. 33, no. 9, pp. 629–808, 2013.  
 [4] A. J. Sinclair, A. Sturrock, B. Davies, and M. Matharu, “Headache management: pharmacological approaches,” *Pract. Neurol.*, vol. 15, no. 6, pp. 411–423, 2015.

[5] H.-C. Diener, A. Charles, P. J. Goadsby, and D. Holle, “New therapeutic approaches for the prevention and treatment of migraine,” *Lancet Neurol.*, vol. 14, no. 14, pp. 1010–1022, 2015.  
 [6] P. Martelletti *et al.*, “Neuromodulation of chronic headaches: position statement from the European Headache Federation.,” *J. Headache Pain*, vol. 14, no. 1, p. 86, Oct. 2013.  
 [7] E. Salkim, A. N. Shiraz, A. Demosthenous, “Effect of Nerve Variations on the Stimulus Current Level in a Wearable Neuromodulator for Migraine :A Modeling Study,” 2017, pp. 239–242.  
 [8] M. I. Iacono *et al.*, “MIDA: A Multimodal Imaging-Based Detailed Anatomical Model of the Human Head and Neck,” *PLoS One*, vol. 10, no. 4, p. e0124126, Apr. 2015.  
 [9] K. N. Christensen, N. Lachman, W. Pawlina, and C.L. Baum, “Cutaneous Depth of the Supraorbital Nerve,” *Dermatologic Surg.*, vol. 40, no. 12, pp. 1342–1348, 2014.  
 [10] K.-J. Shin, H. J. Shin, S.-H. Lee, W.-C. Song, K.-S. Koh, and Y.-C. Gil, “Emerging Points of the Supraorbital and Supratrochlear Nerves in the Supraorbital Margin With Reference to the Lacrimal Caruncle,” *Dermatologic Surg.*, vol. 42, no. 8, pp. 992–998, 2016.  
 [11] C. C. McIntyre, A. G. Richardson, and W. M. Grill, “Modeling the excitability of mammalian nerve fibers: influence of afterpotentials on the recovery cycle.,” *J. Neurophysiol.*, vol. 87, no. 2, pp. 995–1006, 2002.  
 [12] M. L. Hines and N. T. Carnevale, “The NEURON simulation environment.,” *Neural Comput.*, vol. 9, no. 6, pp. 1179–1209, Aug. 1997.  
 [13] T. Yamamoto and Y. Yamamoto, “Electrical properties of the epidermal stratum corneum,” *Med. Biol. Eng.*, vol. 14, no. 2, pp. 151–158, 1976.  
 [14] V. De Santis, X. L. Chen, I. Laakso, and A. Hirata, “An equivalent skin conductivity model for low-frequency magnetic field dosimetry,” *Biomed. Phys. Eng. Express*, vol. 1, no. 1, p. 15201, 2015.  
 [15] C. Gabriel *et al.*, “The dielectric properties of biological tissues: I. Literature survey,” *Phys. Med. Biol.*, vol. 41, no. 11, pp. 2231–2249, Nov. 1996.  
 [16] T. F. Oostendorp, J. Delbeke, and D. F. Stegeman, “The conductivity of the human skull: Results of in vivo and in vitro measurements,” *IEEE Trans. Biomed. Eng.*, vol. 47, no. 11, pp. 1487–1492, Nov. 2000.  
 [17] S. B. Baumann, D. R. Wozny, S. K. Kelly, and F. M. Meno, “The electrical conductivity of human cerebrospinal fluid at body temperature,” *IEEE Trans. Biomed. Eng.*, vol. 44, no. 3, pp. 220–225, Mar. 1997.  
 [18] R. N. Holdefer, R. Sadleir, and M. J. Russell, “Predicted current densities in the brain during transcranial electrical stimulation.,” *Clin. Neurophysiol.*, vol. 117, no. 6, pp. 1388–97, Jun. 2006.